AD-A183 625 A SINGLE ELEMENT CHARGE INJECTION DEVICE AS A SPECTROSCOPIC DETECTOR(U) ARIZONA UNIV TUCSON DEPT OF CHEMISTRY J V SWEEDLER ET AL. 26 MAY 87 TR-40 1/1

UNCLASSIFIED N00014-86-K-0316 F/G 9/1 NL

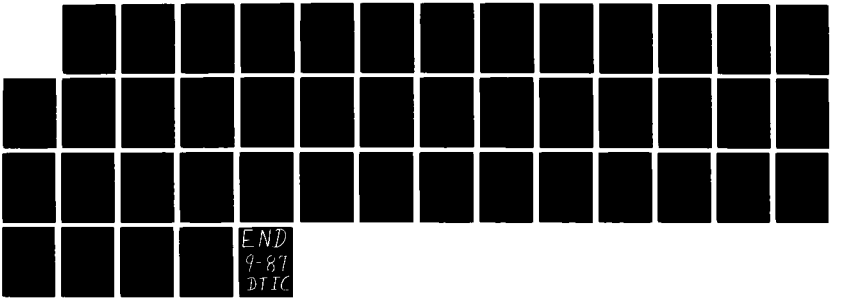

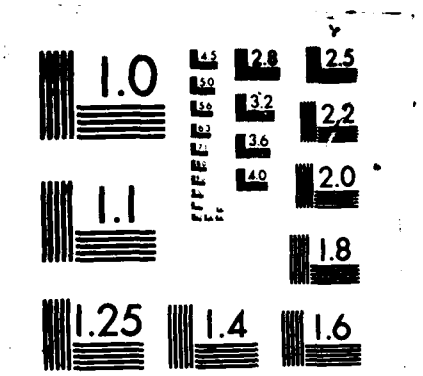

SECURITY CLASSIFICATION OF THIS PAGE (When Data Entered)

REPORT DOCUMENTATION PAGE

READ INSTRUCTIONS BEFORE COMPLETING FORM

1. REPORT NUMBER: 48	2. GOVT ACCESSION NO.
3. RECIPIENT'S CATALOG NUMBER	
4. TITLE (and Subtitle): A Single Element Charge Injection Device as a Spectroscopic Detector	5. TYPE OF REPORT & PERIOD COVERED: Interim
6. PERFORMING ORG. REPORT NUMBER	
7. AUTHOR(s): Jonathan V. Sweedler, M. Bonner Denton, Gary R. Sims, and Richard S. Aikens	8. CONTRACT OR GRANT NUMBER(s): N00014-86-K-0316
9. PERFORMING ORGANIZATION NAME AND ADDRESS: Department of Chemistry, University of Arizona, Tucson, AZ 85721	10. PROGRAM ELEMENT, PROJECT, TASK AREA & WORK UNIT NUMBERS: NR 051-549
11. CONTROLLING OFFICE NAME AND ADDRESS: Office of Naval Research, Arlington, Virginia 22217	12. REPORT DATE: May 26, 1987
	13. NUMBER OF PAGES: 42
14. MONITORING AGENCY NAME & ADDRESS(if different from Controlling Office)	15. SECURITY CLASS. (of this report): Unclassified
	15a. DECLASSIFICATION/DOWNGRADING SCHEDULE

16. DISTRIBUTION STATEMENT (of this Report)

This document has been approved for public release and sale; its distribution is unlimited.

17. DISTRIBUTION STATEMENT (of the abstract entered in Block 20, if different from Report)

18. SUPPLEMENTARY NOTES

Submitted to Opt. Eng. for publication.

19. KEY WORDS (Continue on reverse side if necessary and identify by block number)

Charge injection device, charge transfer device, spectroscopic detector

20. ABSTRACT (Continue on reverse side if necessary and identify by block number)

The need for a single element charge transfer device as a spectroscopic detector is discussed. Such a detector promises to offer superior performance compared to current photomultiplier tubes over a wide range of illumination levels. As a detector to address this need, the prototype CID75 manufactured by General Electric Co. is described and characterized. The CID75 is a single element CID sensor with a 1mm by 1mm photoactive area and a readout rate adjustable from 0 to 20 kHz. The electro-optical

(Continued on other side)

DD FORM 1 JAN 73 1473 EDITION OF 1 NOV 65 IS OBSOLETE
S/N 0102-LF-014-6601

SECURITY CLASSIFICATION OF THIS PAGE (When Data Entered)

20. Abstract (continued)

cont'd → characteristics reported in this study include linearity, read noise, full well capacity, dark count rate, and quantum efficiency. The sensors have good photometric linearity with a full well capacity in excess of 1.2×10^5 electrons. The read noise of the detector can be lowered to 80 electrons when employing the nondestructive readout mode of the CID. The quantum efficiency of the CID75 is reported for the wavelength range of 200-1000 nm. Combining a 10^6 simple dynamic range with the ability to vary integration times over four orders of magnitude allows this detector to quantify photon fluxes varying over ten orders of magnitude. The conclusions of this study are that the CID75 sensor is a useful detector for a variety of applications.

OFFICE OF NAVAL RESEARCH

Contract N00014-86-K-0316

Task No. 051-549

TECHNICAL REPORT NO. 48

A Single Element Charge Injection Device as a Spectroscopic Detector

by

Jonathan V. Sweedler, M. Bonner Denton,

Gary R. Sims, and Richard S. Aikens

Prepared for publication in

Opt. Eng., CCD Issue

Department of Chemistry
University of Arizona
Tucson, Arizona 85721

May 26, 1987

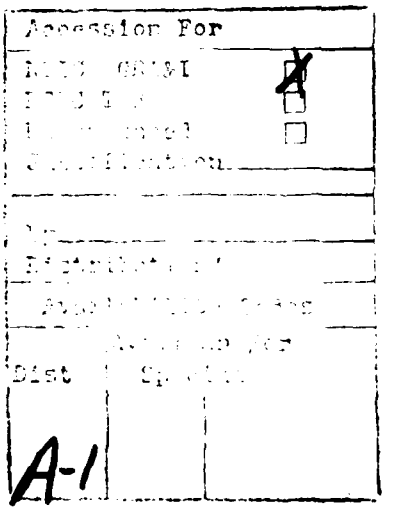

A Single Element Charge Injection Device as a Spectroscopic Detector

Jonathan V. Sweedler, M. Bonner Denton

Chemistry Department

University of Arizona

Tucson, AZ 85721

Gary R. Sims, Richard S. Aikens

Photometrics Ltd.

2010 N. Forbes Blvd. Suite 103

Tucson, AZ 85745

ABSTRACT

The need for a single element charge transfer device as a spectroscopic detector is discussed. Such a detector promises to offer superior performance compared to current photomultiplier tubes over a wide range of illumination levels. As a detector to address this need, the prototype CID75 manufactured by General Electric Co. is described and characterized. The CID75 is a single element CID sensor with a 1mm by 1mm photoactive area and a readout rate adjustable from 0 to 20 kHz. The electro-optical characteristics reported in this study include linearity, read noise, full well capacity, dark count rate, and quantum efficiency. The sensors have good photometric linearity with a full well capacity in excess of 1.2×10^8 electrons. The read noise of the detector can be lowered to 80 electrons when employing the nondestructive readout mode of the CID. The quantum efficiency of the CID75 is reported for the wavelength range of 200-1000 nm. Combining a 10^6 simple dynamic range with the ability to vary integration times over four orders of magnitude allows this detector to quantify photon fluxes varying over ten orders of magnitude. The conclusions of this study are that the CID75 sensor is a useful detector for a variety of applications.

Subject Terms:

charge injection device, charge transfer device, spectroscopic detector

CONTENTS:

1. INTRODUCTION:

Visible and ultraviolet optical spectroscopy today is one of the most widely employed analytical techniques used to routinely characterize the chemical and physical nature of an ever increasing range of materials for science and engineering. During the last twenty years, most of the major improvements in absorption, fluorescence, and emission techniques have involved the development of better sources, absorption cells, wavelength descrimination systems and data reduction systems.

One particularly demanding area involves inductively coupled plasma atomic emission spectrometry (AES). This technique has become a widely accepted method for multielement chemical analysis (1,2). A wealth of information is contained in the spectroscopic signal, including many atomic and ionic emmision lines from most elements in the sample. AES is highly sensitive and has the ability to measure the elements present in the sample over a wide range of concentrations ranging from the percentage level to the high parts per trillion. Two major approaches to designing a AES spectrometer exist, one involving simultaneous multiwavelength monitoring with multiple detectors or an imaging detector array, and the other using a scanning instrument with a single channel detector (1). Currently, the universal detector for scanning AES systems is the photomultiplier tube (PMT). The authors intent is to explore new detector technology to improve AES performance over conventional PMT detection.

The requirements imposed on a detector for a scanning AES system are severe and include the ability to quantify spectral intensities ranging over eight orders of magnitude. The longest practical observation times are on the order of one hundred seconds due to ICP source fluctuations and drift;

therefore, a low dark count rate is not as crucial as in some applications. This manuscript describes the electro-optical evaluation of a new single element charge transfer device (CTD), with an emphasis on the evaluation of the properties which are pertinent to AES. However, this single element CTD has application not only to AES, but to many other areas of spectroscopy and photometry which require a sensitive, wide dynamic range detector.

Most analytical spectroscopists still regard the PMT detector as state of the art in low light level single channel optical detection. The PMT does have many attributes which make it a choice detector for many types of spectroscopy (3-5). Despite the overall good performance and the tremendous success of the PMT, this detector has many limitations:

(1) Low quantum efficiency. The best possible quantum efficiency at the wavelength of maximum sensitivity for a PMT is on the order of 30%. More typical values are on the order of 5% - 20% (5). At wavelengths longer than 900 nm, quantum efficiencies (QEs) are below 1%.

(2) Limited Spectral Range. While it is possible to construct photocathodes optimized for maximum response within nearly any UV-visible wavelength region, no one photocathode is yet available which has high quantum efficiency throughout the ultraviolet to near infrared wavelength range.

(3) High Dark Count Rates. The best performance achievable from individually selected photon counting PMTs, operated under optimal conditions in a cooled chamber, is 4-30 counts/second. This characteristic degrades rapidly as photocathode materials are optimized for the red and near infrared.

(4) Fragile and sensitive to light shock. Exposing a PMT to typical room light conditions while the detector is operating will often destroy it.

Select photon counting PMTs are even more sensitive in that exposing these detectors to even moderate light levels will cause a dramatic and usually irreversible increase in dark count rate (5). For most PMTs, this later problem can occur even with no power applied to the tube.

In addition to these major performance limitations, PMTs have a number of other disadvantages when compared to silicon detectors. They require high voltage power supplies, are bulky, fragile, have finite lifetimes and have large variations in performance between similar devices. Photomultiplier tubes are difficult to use in environments with strong or changing electric or magnetic fields. In addition, they suffer from a number of spurious effects such as nonuniform pulse height distributions, hysteresis effects, and photocathode nonuniformities (5).

These deficiencies point out the need for a superior detection system for single channel applications. Current CTDs (CCDs and CIDs) have many advantages compared to PMTs which make them attractive detectors for spectroscopy. These CTDs are available in a wide variety of formats ranging from over 3,500 element linear arrays, 512 by 512 arrays, to the largest solid state imager of any kind, the Tektronix 2048 by 2048 array (6-8). These solid state array detectors do not suffer from light shock, have low power consumption and are extremely rugged.

In addition, many CTDs offer superior performance compared to PMTs for low light situations on a single detector basis, not even allowing for the huge multiplex advantage that they offer. The performance advantage of CTDs can occur for two reasons. First, the silicon devices have inherently higher quantum efficiencies than the photocathode materials employed in PMTs. Second, the rate of thermal generation of charge carriers can be reduced to insignificant levels by cooling CTDs (8-10), while dark count

rates of approximately four counts per second are currently the limit for photon counting PMTs (5,11). CTDs have the disadvantage of having a finite read noise, the signal independent noise associated with reading the charge information, while for photon counting PMTs the read noise can be less than a single count. Depending on the particular situation, the magnitude of the CTDs read noise, the PMTs dark count rate, and the QEs of the two devices, CTDs will often have higher signal to noise ratios (SNRs) than PMTs. This is true especially in situations where the ability to integrate charge for long periods allows the CTDs to outperform the PMTs.

Many spectroscopic and photometric applications such as a scanning AES system require only a single channel detector. Because of the numerous advantages of CTDs, a logical step is to make a large single element detector to replace photomultiplier tubes for these single channel applications. A CTD designed as a direct replacement for a photomultiplier tube should have a comparable photoactive area. Several approaches to using a CTD as a photomultiplier tube replacement exist. The most obvious and simple approach is to use a single large element CTD. In addition to a single large element CTD, a small array detector such as the Texas Instruments TC211 CCD is well suited for such an application. The multiple detectors result in no loss in performance as compared to a single large detector by using binning under low light level situations and reading each detector element individually under high light level situations. It is conceivable that either of these two approaches can lead to a single channel detector with a good quantum efficiency from 190-1000 nm, a dark count rate on the order of one count per second, a dynamic range of measurable photon fluxes (spectral line intensities) of over ten orders of magnitude, with a

minimum detectable signal of approximately one photon per second with sufficient integration times.

Interaction with the engineering staff at General Electric has resulted in the development of a single element charge injection device (CID) detector. The operating principles of this device are similar to the more conventional charge injection device imaging arrays in that charge is generated and stored in an epitaxial n doped silicon layer by the absorption of photons. The accumulated charge is then measured via an intracell charge transfer process (12-14). The unique feature of this readout mechanism is that the charge measurement process is either nondestructive, i.e. the quantity of charge in the sensor is not altered during measurement and can thus be repeatedly determined, or destructive, i.e. the charge is removed.

The availability of this unique single element sensor specifically designed as a PMT replacement was the driving force behind the use of CID rather than CCD technology. Previous work in our laboratories using more conventional CID array detectors indicate that the single element CID has the performance required of a detector for AES. This paper presents an evaluation of the spectroscopically important characteristics of this new detector, including system read noise, full well capacity, linearity, dynamic range, QE from 200-1000 nm, and dark count rate.

2. EXPERIMENTAL:

2.1 Description of CID75:

The single element CID75 used in these tests is manufactured by General Electric. The CID75 is made using the same fabrication process as other GE CIDs. The sensor consists of two polysilicon capacitors; to maximize sensitivity and minimize electrical crosstalk, each capacitor consists of a

set of very narrow, widely spaced electrodes. The spacing between electrodes has been adjusted to match the diffusion length of minority carriers at reduced temperatures. These electrodes are arranged in an grid pattern separated from an n doped silicon epitaxial layer with a silicon oxide insulator. The electrodes are biased to form an inversion region in the epitaxial region where the photogenerated charge is collected as illustrated in Fig. 1. While the minority carriers in the n doped silicon are holes, the photogenerated charge will be referred to as electrons throughout this report. The photogenerated charge is sampled by changing the bias on the two electrodes in order to transfer the charge between the electrodes. The charge is cleared from the sensor by removing the bias from both electrodes simultaneously. Fig. 2 shows the arrangement of the capacitors, along with a simplified schematic of the off-chip preamplifier. References 12-18 describe in much greater detail the structure, operation and read modes of CIDs.

Several aspects of the CID are well suited for spectroscopic applications. The nondestructive readout mode of the CID allows charge information to be read as many times as desired. By averaging successive nondestructive readouts (NDROs), the effective read noise of the system can be greatly reduced. The nondestructive readout mode also allows variable integration time exposures to be made without prior knowledge of the photon flux. Approximately 80% of the surface of the CID is exposed to incident radiation, with the rest covered by the polysilicon electrodes. Thus, the QE of the device is high compared to many front-side illuminated CTDs.

2.2 The UA CID75 System

The CID75 is a prototype device and no evaluations of its operating characteristics and electro-optical properties have been previously performed. A detector system was designed for this sensor based on the design of a two dimensional CID camera developed in our laboratories (13-14). This system consists of three main sections: the sensor Dewar, sensor head and a system computer.

The CID Dewar assembly consists of a liquid nitrogen cryostat, temperature regulating and monitoring electronics, a CID preamplifier card, and the CID. To allow cooling of the CID75 to temperatures of approximately 130 K, the CID is located in a Dewar evacuated to less than 0.1 mtorr. The preamplifier used for the CID is a charge amplifier with a gain corresponding to 30 nV per electron. This gain was chosen to allow sampling of the upper end of the detectors dynamic range. The output of the preamplifier is fed into a modified Photometrics Ltd. analog card which contains the amplification, processing, filtering and 14 bit digitization circuitry (19).

Because many of the operating characteristics of the CID are temperature dependent, such as the rate of thermal charge generation and the surface interface trap exchange rate, it is important to be able to precisely measure the temperature of the sensor. The temperature is measured by passing a constant current through a diode located on the CID75, and measuring the voltage drop across the diode; the voltage drop is linearly related to the temperature over the temperature range of CID operation. The CID is cooled by contact with a copper cold finger connected to the liquid nitrogen cryostat. The temperature monitoring system is

disconnected from the system during most experiments to eliminate light emission caused by forward biasing the temperature diode.

In addition to the analog electronics, the sensor head contains circuitry to generate the proper voltages and waveforms for operation. Because of the lack of the select and deselect scanners and other multiplexing circuitry present in the two dimensional CID arrays, the required waveforms to run this device are simple. The drive and inject lines are the only two clocks required to run the CID; however, six other lines are used to perform the correlated double sampling, filtering, adjustable gain, and analog to digital conversion. In order to provide noise free inputs to the CID Dewar, all the signals are opto-isolated and the electronics are carefully shielded. The 14 bit digitized data is sent to the host computer, a PDP 11-03. All software is written in CONVERS, a FORTH like threaded code interpretive compilier developed in these laboratories to facilitate instrumentation control and data analysis.

2.3 Test Systems:

A variety of the evaluations of device performance were conducted using a simple test apparatus consisting of a capped, cylindrical, aluminum test jig, the inside of which is coated with high reflectance paint. A ring of five light emitting diodes (LEDs) inside the cylinder is used as a light source, with the duration of illumination controlled by computer. In order to avoid the effects of junction heating on light output of the LEDs, they are turned on for 500 ns with a precision exceeding 10 ns, with a cool down time of approximately 5 μs between flashes. The amount of light reaching the detector is precisely and reproducibly controlled by flashing the LEDs the desired number of times. The precision in controlling the illumination by turning the LEDs on and off using the computer is greater than the precision obtainable with a mechanical shutter.

QE measurements from 200-1000 nm were made using a GCA McPherson monochromator with a combination of deuterium and tungsten sources. The output of the monochromator enters a 10 cm diameter integrating sphere, and the CID is illuminated through a 2 cm port in the integrating sphere. A series of interference and long pass filters are placed between the monochromator and integrating sphere to eliminate stray light and second order radiation from reaching the detector. The light intensity as a function of wavelength at the focal plane of the spectrometer is precisely measured using an EG&G photodiode with a calibration traceable to the National Bureau of Standards. The methods used to measure the quantum efficiency have been extensively reported elsewhere (14,19).

3. EVALUATION OF ELECTRO-OPTICAL PROPERTIES:

3.1 Determination of System Gain by Mean-Variance Measurements

Before an evaluation of the electro-optical characteristics of this sensor are undertaken, the quantity of charge which produces a given analog to digital count (system gain) must be accurately known. A value for the system gain is important or the results of measurements such as the dark count rate in units of ADUs per second can not be related to the fundamental units of electrons per second. In order to make an accurate determination of the system gain for the UA/CID75 detector system, the mean variance (photon transfer) method was used (8,9,13,20).

This technique utilizes the fact that photon detection obeys Poisson statistics. In a Poisson distribution, the mean of the distribution is equal to the variance of the distribution (21). Using this relationship and relating the mean and variance measured in units of ADUs with the fundamental mean and variance with units of electrons, one obtains the following equation:

$$S_s^2 = G * \bar{N} \qquad (1),$$

where S_s is the standard deviation of the signal due to shot noise (ADUs), G is the system gain (ADUs/electron), and $\bar{N}$ is the mean signal (ADUs). Eq. (1) indicates that G, the system gain, can be calculated if the signal level and variance in the signal due to shot noise are known. However, shot noise is not the only noise source associated with determining the number of incident photons. The noise associated with reading out the detector (system read noise) must also be taken into account in Eq. (1). It is

important to note that the system read noise is due to various noise sources in the detector and amplifier which are independent of the quantity of charge in the detector. The net variance from the the shot noise and read noise is

$$S_t^2 = G * \bar{N} + S_r^2 \qquad (2),$$

where S_t^2 is the total observed variance $(ADUs)^2$, and S_r^2 is the variance from the read noise $(ADUs)^2$. When the sensor is exposed to light in a series of increasing exposures and the mean and variance are determined at each illumination level, a plot of the mean signal in ADUs versus the total variance in $ADUs^2$ yields a straight line with a slope of G and intercept of S_r^2.

The mean variance measurements on the UA/CID75 camera system were conducted using the test apparatus described in section 2.2. At each illumination level, the CID was read, LEDs were flashed the appropriate number of times, and the CID read again. Each CID readout was the average of 16 NDROs; the use of 16 NDROs reduces the system read noise and thus allows a more accurate value for the system gain to be calculated. The mean and variance are calculated from 128 reads, with the entire process repeated at 40 levels of illumination covering the linear operating range of the CID. The slope of the best line through these points was determined with a least-squares fit to be 74.3 electrons/ADU with a standard deviation of 2 electrons/ADU.

3.2 System Read Noise

For spectroscopic detectors, many of the interesting signals are of low magnitude and the noise of the detector at these low illumination levels limits the overall performance. For many other spectroscopic applications a large dynamic range is important, and since the read noise usually determines the lower end of the dynamic range, a low read noise is important for these applications also. The system read noise is the sum of all noise sources other than photon and dark current shot noise, and can be separated into the noises from the sensor, and noise sources from the external amplifier and drive circuitry. A major noise source in CIDs has been attributed to Johnson noise from resistance in overlaying gate electrodes, and the high capacitance of the sense electrode (23). The major sources of noise in the off-chip preamplifier used in this system include Johnson noise from the channel resistance of the input FET, shot noise from leakage currents in the input FET, and 1/f noise (22). The use of the correlated double sampling scheme eliminates most of the noise contributions from KTC (switch) noise.

Voltage spikes and ripple on the drive line couples into the CID sense line adding another noise source. The capacitive coupling of the drive and sense electrodes on the CID of <1pf causes a significant coupling of the drive signal to the sense line. To minimize this effect, a capacitance similar to the drive-sense capacitance is inserted between the drive line and the noninverting input of the off-chip charge amplifier as shown in Fig. 2. By carefully matching these capacitances, over 98% of the drive-sense coupling signal is rejected.

The read noise of the UA/CID75 detector system is measured using the mean variance method discussed in the last section. As shown by Eq. 2, the intercept of a mean variance plot is S_r^2, the system read variance. Using this method, the read noise is calculated to be 6 ADUs/read. This corresponds to 450 electrons per read using the value of gain calculated in section 3.1.

An advantage of the nondestructive read capability of the CID is the ability to reduce the system read noise by averaging signals from a number of nondestructive reads. If the read noise is white and is uncorrelated from one read to the next, the effective noise floor will be reduced by the square root of the number of NDROs. In practice, it is not expected that the reduction will be this great since the limited bandwidth of the video amplifiers and 1/f noise both limit the effectiveness of this type of signal averaging. The effective read noise was measured using the mean variance method described above with varying numbers of NDROs. A large decrease in the effective read noise is observed as the number of reads increases, with the read noise being reduced to under 80 electrons with 400 NDROs.

3.3 Linearity

One requirement for a spectroscopic detector is that it have a well defined response to radiation which can be related to the total number of incident photons. The charge sensing preamplifier used in the UA/CID75 system is expected to produce a signal linearly proportional to the quantity of charge in the detector. The response of the CID75 to radiation measured over a wide range of illumination levels is shown in Fig. 3a. The upper end

of the linearity plot occurs when the sensor has reached saturation at over $1.2x10^8$ electrons.

A detail of the linearity is shown in Fig. 3b for illumination levels up to $5x10^6$ electrons. One feature of the response shown in Fig. 3b is the nonlinear "foot". The foot of the plot is attributed to the filling of charge trap sites in the $Si-SiO_2$ interface (13,23). Because of these traps, the first charge generated in the detector is held by these traps and is unable to move from the charge collection capacitor to the charge sensing capacitor. Interface traps are common to all surface channel MOS detectors such as CIDs and surface channel CCDs, and to a lesser extent in buried channel CCDs. A technique to avoid the nonlinear operating region in such detectors is to introduce a bias charge, sometimes called a "fat zero," to fill the interface traps. Once the interface trap states are occupied, all further charge added to the detector is mobile and gives a linear response function. The nonlinear foot in the CID75 amounts to over $2x10^5$ electrons. The linear portion of the plot is for exposures between $2x10^5$ and $1.2x10^8$ electrons. The maximum deviation from linearity, expressed as the maximum deviation from the best fit line divided by the full well capacity, is under 0.1%.

3.4 Dark Count Rate:

One of the major potential applications for the CID75 sensor is in low light level, long exposure situations. If the thermal generation rate can not be sufficiently reduced by cooling, then the shot noise present on the thermally generated charge limits the minimum detectable signal. The

thermal generation of charge, often called dark current, is due to electron-hole pair generation by midgap defects in the bulk semiconductor and at the $Si-SiO_2$ interface (24). In surface channel CTDs, the dominant source of dark current is from interface states at the $Si-SiO_2$ interface (25). The thermal generation rate was determined by taking long integration time exposures. The dark current at 130 K is 100 electrons per second. With a dark count rate of 100 electrons per second, the shot noise from a two minute integration introduces 110 electrons of noise. The large area of the single element in the CID75 contributes to the high dark count rate of 100 electrons per second; its dark current of 10 nA/cm^2 at 23 C is similar to values for other CTDs (8). Operating the sensor at temperatures lower than 130 K may reduce the dark count rate further. It also may be possible to reduce the dark count rate by raising the potential of the sense line during integration to form an inversion layer under the sense capacitor. This suppresses the thermal generation of charge from surface interface states (25). Both of these methods are being examined to determine their effectiveness in further reducing the dark count rate.

3.5 Spectral Response:

The sensitivity of a detector at any given wavelength is one of the most important parameters when a particular device is being considered for a specific spectroscopic application. The QE (electrons collected and measured per incident photon) of the CID75 in the near infrared to ultraviolet range was measured. The quantity of charge generated in the sensor during a known integration period due to photons from a monochromatic source of known flux is determined at each wavelength.

The sensitivity of the sensor strongly depends on the optical properties of the silicon epitaxy, overlaying gate electrodes and oxide layers. The QE of silicon CTDs falls off rapidly in the near infrared due to the decreasing absorption coefficient of silicon at longer wavelengths. As the absorption coefficient decreases, photons are either absorbed deep in the epitaxy or pass entirely through the epitaxy and are absorbed in the bulk silicon. The CID can not respond to photons with less energy than the band gap of silicon (approximately 1200 nm at 300 K). The photogenerated charge deep in the epitaxy is more likely to undergo charge recombination before being collected. The decreased sensitivity of a CID for ultraviolet wavelengths is due to photon absorption and reflection from the silicon oxide layer and the multiple polysilicon electrodes overlaying the epitaxy.

The method used to measure the QE is given in section 2.3 and has been reported in the literature (14,19). The results of the quantum efficiency measurements of the CID75 detector from 200-1000 nm are shown in Fig. 4. The QE curve has a broad maximum of 34% centered around 550 nm and another region of high sensitivity at 250 nm of 35%. The ultraviolet QE of this device is high compared to other CID sensors (14) and three phase front-side illuminated CCD detectors (19) because of less overlaying gate structure.

3.6 Dynamic Range:

For many spectroscopic techniques such as AES, the range of analytically useful photon fluxes varies over many orders of magnitude. If a detector is not to limit these techniques a very large dynamic range is required. The simple dynamic range (SDR) of a CTD detector is defined as the ratio of the full well capacity to the read noise. Of greater importance to the spectroscopist is the range of photon fluxes the detector

is able to quantify. For the purposes of these discussions, the photon flux dynamic range (PFDR) is the ratio of the highest and lowest photon fluxes which can be accurately measured with variable integration times. The PFDR depends on a number of factors, many which depend on the intrinsic abilities of the detector and others which depend on the particular detector system and configuration.

The lower end of the PFDR is set by a number of factors including the length of observation, dark count rate, quantum efficiency and system read noise. The minimum detectable signal is defined as the photon flux which yields a SNR of 2. Examining the linearity curve in Fig. 3b, it is apparent that the CID has an extremely nonuniform response to illumination levels under 2×10^5 electrons. To achieve a linear response function at low illumination levels, a bias charge is introduced.

The nondestructive read ability of the CID allows one to use a bias flash or "Fat Zero" without introducing significant noise. In CIDs and CCDs, the KTC (switch) noise is eliminated by using the correlated double sampling technique (6). While there is an uncertainty in the voltage of resetting the FET dictated by KTC noise, the use of the correlated double sample subtracts out this as an offset. In the CID (but not the CCD), a similar technique is used to eliminate the effect of the fat zero shot noise. This is done by exposing the sensor to several LED flashes to bring the sensor to the linear portion of its dynamic range. After the flash but prior to exposure to the spectroscopic signal, the quantity of charge produced by the bias is determined by reading out the CID. While the number of electrons produced by the bias flash (fat zero) is subject to the uncertainty of shot noise, the number of electrons is fixed and can be determined exactly subject only to the limitations imposed by the system

read noise. After the magnitude of the bias flash has been measured, the CID is exposed, and then read out again. The signal level is the difference between the two correlated reads. Since two reads are required to obtain the useful exposure level, this technique increases the effective read noise by $(2)^{1/2}$. Since the read noise is reduced to 100 electrons with 100 NDROs, the effective read noise is 140 electrons and the minimum detectable signal is 280 electrons.

The maximum practical integration time is dictated by a number of factors including instrument and source stability, signal duration, and patience. For AES and several other spectroscopic techniques, the maximum practical integration time is limited by source stability and is on the order of several minutes. For a two minute exposure and a dark count rate of 100 electrons per second, the thermal generation of charge amounts to 12000 electrons, and thus introduces approximately 110 electrons of noise. The total noise obtained by the addition in quadrature of the dark count noise and two times the read noise is 180 electrons for the 120 second observation time. Therefore, the minimum detectable signal is 3 electrons per second, corresponding to 9 photons per second at 500 nm.

The maximum measurable photon flux is determined by a number of factors including the full well capacity of the detector, the maximum readout rate, the maximum rate that the sensor can be cleared of charge, and the quantum efficiency of the device. For extremely intense spectral features, the nonuniform foot to the photometric response becomes insignificant to the large full well capacity of 10^8 electrons, and hence the bias charge is not needed. In addition, NDROs are not required to reduce the effective system read noise for extremely intense features. The maximum sampling rate is dictated by both the maximum readout rate and the minimum time between the

end of the inject sequence and the start of the read process, which yields an effective maximum sampling rate of approximately 10 kHz. Combining the maximum readout rate of 10 kHz with a charge capacity of 10^8 electrons yields a maximum measurable electron generation rate of 10^{12} per second.

The PFDR of this detector is from under 10 electrons per second to 10^{12} electrons per second. These numbers are related to the numbers of incident photons by taking into account the wavelength dependent quantum efficiency of the device shown in Fig. 4. It is important to realize that these numbers for the dynamic range were obtained using a rather simple method. A number of factors effect the realizable dynamic range in CTDs including latent image and hysteresis effects which can prevent the measuring of extremely weak signals immediately after measuring intense features. However, while not fully experimentally verified, this discussion demonstrates that this detector has a large effective dynamic range and should be useful in a wide variety of large dynamic range applications.

The SDR of this detector is greater than 10^6 and so either a variable gain analog amplifier or a 20 bit A-D is required if the off-chip electronics are not to limit the system performance. In the UA/CID75 system, a variable gain analog chain and a 14 bit A-D are used to allow sampling the entire SDR of the CID75. The nondestructive readout mode of the CID allows for efficient use of this detectors full PFDR by allowing the gain, readout method and integration time to be varied to fit the particular measurement being made. During an exposure, the CID is read nondestructively and if the signal level is below some threshold value, a more sensitive gain setting and longer integration time are used. This process of reading out the sensor nondestructively and selecting the desired

analog gain is repeated until sufficient light has been collected for the desired SNR or until some maximum time has been reached. In this way, the entire A-D process from analog gain to integration time can be tailored for each measurement depending on the photon flux without any prior knowledge of the light intensity.

3.7 Hysteresis Effects

It is important that measurements obtained from a detector are not influenced by the prior operation of the device, such as exposure to intense light, reading the device, injecting the charge of any other type of normal operation. Any such perturbations arising from normal operation are termed hysteresis effects. Hysteresis effects are especially detrimental in spectroscopic applications where a detector must accurately measure light intensity over rapidly changing optical conditions.

Most common spectroscopic detectors, including photomultiplier tubes, suffer from some form of hysteresis effects. Modern solid state detectors such as photodiode arrays (PDAs) and CTDs are fairly resistant to these effects. However, close examination of signals from these devices indicate some dependence on prior operation; for example, residual image effects are common in CCDs. It has been found that the CID also suffers from some forms of hysteresis effects. Clearing the CID of charge, and exposing the CID to bright images both have slight effects on the subsequent performance of the CID11B sensor (14). In addition, work with other CID sensors indicates that under some conditions, the apparent quantity of charge in the sensor can diminish very slightly when an individual detector is repeatedly read in the nondestructive mode. The source of these effects is postulated to be caused by the gradual movement of charge into and out of the $Si-SiO_2$ interface.

In bulk silicon, charge exists in only one of two energy states, the valence band and conduction band. At the Si-SiO_2 interface, there are a number of allowed energy states where charge can reside. Because these energy states are associated with specific physical locations, charge residing in these regions is immobile and is known as "trapped charge". However, charge in a trapped state can gain sufficient energy to move into the conduction band and thus become mobile. The energy of most trapped states is similar to the energy of the conduction band (23), and charge in these states rapidly exchanges with the charge in the conduction band. Because of the rapid interchange, this type of trapped charge is referred to as "fast interface states". A few states are found to be energetically different and to exchange very slowly with the conduction band, with some of these states having time constants of hours at 100 K.

In all the previous discussions, it has been assumed that the nondestructive read mode of the CID is truly nondestructive, i.e. that no charge is gained or lost by the read process. This assumption is not entirely correct. While the sensor is integrating charge, the accumulated charge is only stored under the potential well under the drive electrode. Any charge created in the vicinity of the sense electrode is pulled under the drive electrode because this electrode is biased more negatively. Because all mobile conduction band charge is stored under the drive electrode, the slower trap states under the drive electrode are filled. The sense electrode has no conduction band charge stored under it and hence the slower trap states under this electrode are unfilled. During a nondestructive read, the mobile charge under the drive electrode is shifted under the sense electrode for a short time (between 10-40 μs per read for the UA/CID75 system). While the charge is under the sense electrode, some

trap states are filled. Therefore, when the read is completed, not all of the charge transferred from the drive electrode to the sense electrode returns to the drive electrode. Since the quantity of charge transferred on subsequent reads has been decreased, the measured signal decreases with the number of reads.

In order to measure this phenomenon, the CID was cleared of charge and then exposed to light to create approximately 3.6×10^7 electrons. The CID was then left idle for ten minutes in order to allow the trap states under the drive electrode to reach equilibrium. Then the sensor was read and the observed signal plotted as a function of read number in Fig. 5. The first read is 0.8×10^6 electrons higher than the second read, and after 30 reads, a total of 10^6 electrons are lost. Several thousand additional reads have little effect on the signal, with the signal changing by less than 10^3 electrons (<0.01%) from reading out the sensor an additional 1000 times. While this effect is significant, the change in signal level caused by the nondestructive read process can be almost completely eliminated by simply discarding the data from the first several reads of the detector.

In addition to effecting the nondestructive read process, the slow trap states cause a change in observed signal due to the adsorption and reemission of mobile charge from these sites after exposure of the sensor to changing illumination levels. This effect has been extensively characterized in the CID118 detector (14). Preliminary studies on this type of hysteresis effect in the CID75 indicates that this effect, in worst case situations (such as leaving the sensor in the dark for prolonged periods and then exposing the detector to very intense illumination levels), causes the signal level to change by approximately 0.3% with time. Additional studies

are currently underway to investigate the role of trapped charge on the response of the CID75.

3.8 Charge Injection Efficiency

In CCDs, the charge readout process also clears the detector of charge. In CIDs, the charge readout and charge clearing (injection) process are independent. In order to measure and optimize the charge injection process, the CID is exposed to a preset charge level (usually corresponding to approximately 4×10^7 electrons). To clear the CID75 of charge, both the drive and sense electrodes are set to a potential approximately the same as the epitaxial layer potential, causing the electrons to recombine with the stored positive charge. The length of time the drive and sense electrodes were left at the epitaxy potential ranged from 10-10,000 μs. It was found that only 30% of the charge was removed regardless of the length of the inject cycle or the numbers of inject cycles performed. Reading out the device between each inject cycle greatly increased the efficiency of the charge injection process. The charge clearing process appears to preferentially remove a fraction of the photogenerated charge, and longer or repeated inject cycles remove no further charge. However, reading the device between each inject reestablishes an equilibrium distribution of charge carriers, allowing further charge to be removed. Fig. 6 shows the charge contained in the sensor as a function of the number of inject-read cycles. After eight of these cycles, the CID is quantitatively cleared of all charge.

As well as removing the charge from the conduction band, the combination inject-read process also appears to remove the charge from most trap sites. Thus the first charge created after the CID is cleared of

charge goes into the trap sites because they are lower in energy than the conduction band. The trap sites are normally filled with bias charge in order to allow subsequently generated charge to be mobile (see linearity section 3.3).

4. CONCLUSIONS:

The CID75 sensor appears to fulfill many of the needs of a spectroscopic detector. Table 1 is a summary of these evaluation results. The $1mm^2$ photoactive area makes this sensor very easy to use in many applications. The sensitivity of the detector is good over a wide spectral range. The detector has a linear response over a wide range of illumination levels; the NDRO ability of the CID allows a bias flash to be used to eliminate the effects of a nonlinear response at low light levels without introducing significant noise. The dark count rate, while not insignificant, is low enough for AES and many other applications. In fact, a several week long exposure is required to saturate the device from dark current alone. The low readout noise, coupled with the large full well capacity give this detector a large simple dynamic range. The most striking feature of this detector is its extremely large PFDR; using the nondestructive read mode of this detector and the ability to vary the integration time of the detector from microseconds to minutes, this detector can measure photon fluxes ranging over ten orders of magnitude.

The CID75 should offer significant improvements in performance over the PMT as an AES detector. Of prime importance is the wider PFDR and the comparable sensitivity to PMTs. Also significant, the CID75 allows the use of spectral lines over the wavelength range from 200-1000 nm. The very near infrared spectral region (800-1000 nm) holds much promise for AES of nonmetals (26-27), however, the lack of good detectors in this wavelength region has slowed research in this area. Future work includes determining the responsivity of the sensor in the 140-200 nm range. The availability of

a single detector to cover the entire spectral range of interest for AES (140-1000 nm) is exciting. The UA/CID75 system will be used in these laboratories as an AES detector in the near future.

In addition to AES, other spectroscopic and photometric applications can benefit from the CID75. In UV-Vis Fourier transform spectroscopy, the PFDR of the detector can determine the sensitivity of a measurement, and hence FTS should benefit from the use of this detector. The CID75 has application in situations requiring a detector to function with high sensitivity or large dynamic range in environments with rapidly changing electric and magnetic fields where it is difficult to operate PMTs, and in situations requiring a small size, low power consumption, rugged detector.

While the current UA/CID75 system does not meet all the performance goals for a CTD detector discussed in section 1, the system is capable of achieving high performance as a general purpose spectroscopic detector. The availability of new CIDs and CCDs, with improved and more flexible support sytems promise to offer unparalleled performance for single channel applications. Future work will focus on comparing the merits of CIDs and CCDs for such single element applications.

5. Acknowledgements:

We wish to thank Gerrold J. Michon, Joseph Carbone, Hugh K. Burke and Robert F. Wentink of General Electric Co. for the CID75 sensors, and their help and encouragement in these studies. This work was partially funded by the Office of Naval Research.

6. REFERENCES

1) P.W.M. Boumans, Inductively Coupled Plasma Emission Spectroscopy, Part 1- Methodology, Instrumentation, and Performance, Chemical Analysis v. 90, Wiley, New York (1987).

2) P.W.M. Boumans, Inductively Coupled Plasma Emission Spectroscopy, Part 2- Applications and Fundamentals, Chemical Analysis v. 90, Wiley, New York (1987).

3) R.P. Cooney, G.D. Boutilier, J.D. Winefordner, "Comparison of image devices vs. photomultiplier detectors in atomic and molecular luminescence spectrometry via signal-to-noise ratio calculations," Anal. Chem. 49(7), 1048 (1977).

4) T.M. Niemczyk, D.G. Ettinger, S.G. Barnhart, "Optimization of parameters in photon counting experiments," Anal. Chem. 51(12), 2001 (1979).

5) R.W. Engstrom, Photomultiplier Handbook, RCA Corporation, (1980).

6) E.L. Dereniak and D.G. Crowe, Optical Radiation Detectors, Wiley, New York (1984).

7) M.M. Blouke, D.L Heidtmann, B. Corrie, M.L. Lust, J.R. Janesick, "Large area ccd image sensors for scientific applications," in Solid State Imaging Arrays, K. Prettyjohns, E. Dereniak, eds., Proc. SPIE 570, 82-88, (1985).

8) J.R. Janesick, T. Elliott, S. Collins, H. Marsh, M. Blouke, and J. Freeman, "The future scientific CCD," in State-of-the-Art Imaging Arrays and Their Applications, K. Prettyjohns, ed., Proc. SPIE 501, 2-31, (1984).

9) A. Fowler, P. Waddel, L. Mortara, "Evaluation of the RCA 512x320 charge-coupled device (CCD) imagers for astronomical use," in Solid State Imagers for Astronomy, J. Geary and D. Latham, eds., Proc. SPIE 290, 34-44 (1981).

10) M.B. Denton, H.A. Lewis, and G.R. Sims, "Operational characteristics and consideration when employing charge injection and charge coupled devices in practical chemical analysis," ACS Symposium Series No. 236, 133 (1983).

11) B.H. Candy, "Photomultiplier characteristics and practice relevant to photon counting," Rev. Sci. Instrum. 56(2), 183 (1985).

12) H.A. Lewis, M.B. Denton, "Determination of the ultraviolet and visible response of a charge injection device array detector," J. Automatic Chem. 3, 9 (1981).

13) G.R. Sims and M.B. Denton, "Simultaneous Multielement Emission Spectrometry using a Charge Injection Device Detector," ACS Symposium Series No. 236, 117 (1983).

14) G.R. Sims and M.B. Denton, "Characterization of a charge injection device camera system as a multichannel spectroscopic detector," J. Opt. Eng., in press.

15) G.J. Michon and H.K. Burke, "Charge injection imaging," IEEE Digest of Technical Papers, 138 (1973).

16) G.J. Michon and H.K. Burke, "Operational characteristics of CID imager," IEEE International Solid State Circuits Conf. 26 (1974).

17) G.J. Michon, H.K. Burke, and P.M. Brown, "Recent developments in CID imaging," Proceedings of Symposium on Charge-Coupled Device Technology for Scientific Imaging Applications, Sponsored by the Jet Propulsion Laboratory, 106-115 (March 6-7, 1975).

18) G.R. Sims and M.B. Denton, "Spatial pixel crosstalk in a charge injection device," J. Opt. Eng., in press.

19) P.M. Epperson, J.V. Sweedler, M.B. Denton, G.R. Sims, T.W. McCurnin, and R.S. Aikens, "Electro-optical characterization of the Tektronix TK512M-011 CCD," J. Opt. Eng., in press.

20) J. Janesick, K. Klaasen, T. Elliot, "CCD charge collection efficiency and the photon transfer technique," in Ultraviolet Technology, R. Huffman, Ed., Proc. SPIE 687, 36-55, (1986).

21) P.R. Bevington, Data reduction and Error Analysis for the Physical Sciences, McGraw-Hill Book Co, (1969).

22) F.A. Sachs, "Solid-State Imaging Systems," Electro-Optical Systems Design 7, 34 (October 1975).

23) G.J. Michon, H.K. Burke, T.L. Vogelsong, and K. Wang, "Noise in Charge Injection Device (CID) Array Imagers," in Recent Advances in TV Sensors and Systems, C.F. Freeman, ed., Proc. SPIE 203, 66 (1979).

24) N.S. Saks, "Interface state trapping and dark current generation in buried channel charge-coupled devices", J. Appl. Phys. 53(3), 1745-1753 (1982).

25) N.S. Saks, "A technique for suppressing dark current generated by interface states in buried channel CCD imagers", IEEE Electron Device Letters EDL-1(7), 131-133 (1980).

26) S.K. Hughes, R.M. Brown, R.C. Fry, "Photodiode Array Studies of C,H,N, and O in the Argon inductively coupled plasma", Appl. Spectrosc. 35, 493, (1981).

27) D.E. Pivonka, W.G. Fateley, R.C. Fry, "Simultaneous determination of C,H,N,O,F,Cl,Br and S in gas chromatographic effluent by Fourier transform red/near-infrared atomic emission spectroscopy," Appl. Spectrosc. 40, 291, (1986).

FIGURE CAPTIONS

Figure 1: Cross section of the CID75 showing the drive and sense electrodes. The photoactive area of this single element detector is 1mm by 1mm.

Figure 2: A top view of the CID75 sensor showing the grid like arrangement of the drive and sense electrodes. Also shown is a simplified schematic of the charge amplifier used in these studies. The entire preamplifier is contained in the vacuum cryostat in close proximity to the sensor. The capacitor between the drive line and the noninverting input of the operational amplifier is used to null out the effect of the drive line capacitively coupling to the sense line.

Figure 3a: Photometric response of the CID75 sensor system demonstrating the linearity of the system. Full well capacity of the CID75 is over 1.2×10^8 electrons.

Figure 3b: Detail of the photometric response of the CID75 for illumination levels up to 5×10^6 electrons. The nonlinear "foot" in this curve is due to surface interface traps. See text for discussion.

Figure 4: The QE of the CID75 detector from 200-1000 nm. The peak QEs are 34% at 550 nm and 35% at 250 nm.

Figure 5: The output of the sensor as a function of the number of NDROs at 130 K. The output of the sensor decreases, with a 2.6% change after 30 NDROs. 1000 additional NDROs have little effect on the output.

Figure 6: Charge injection efficiency, showing the decrease in the amount of charge contained in the sensor as a function of the number of inject-read cycles at 130 K. After eight cycles, the sensor is quantitatively cleared of charge.

Read Noise	450 e^- 80 e^- with 400 NDROs
Linearity	0.1% maximum deviation
Full well capacity	1.2×10^8 e^-
Dark count rate	100 e^-/sec. @ 130 K
Quantum Efficiency	35% @ 250 nm 34% @ 550 nm
Dynamic Range: Simple (SDR) Photon flux (PFDR)	 $>10^6$ $>10^{11}$

Table 1. Summary of General Electric CID75 Electro-optical Performance

CID75

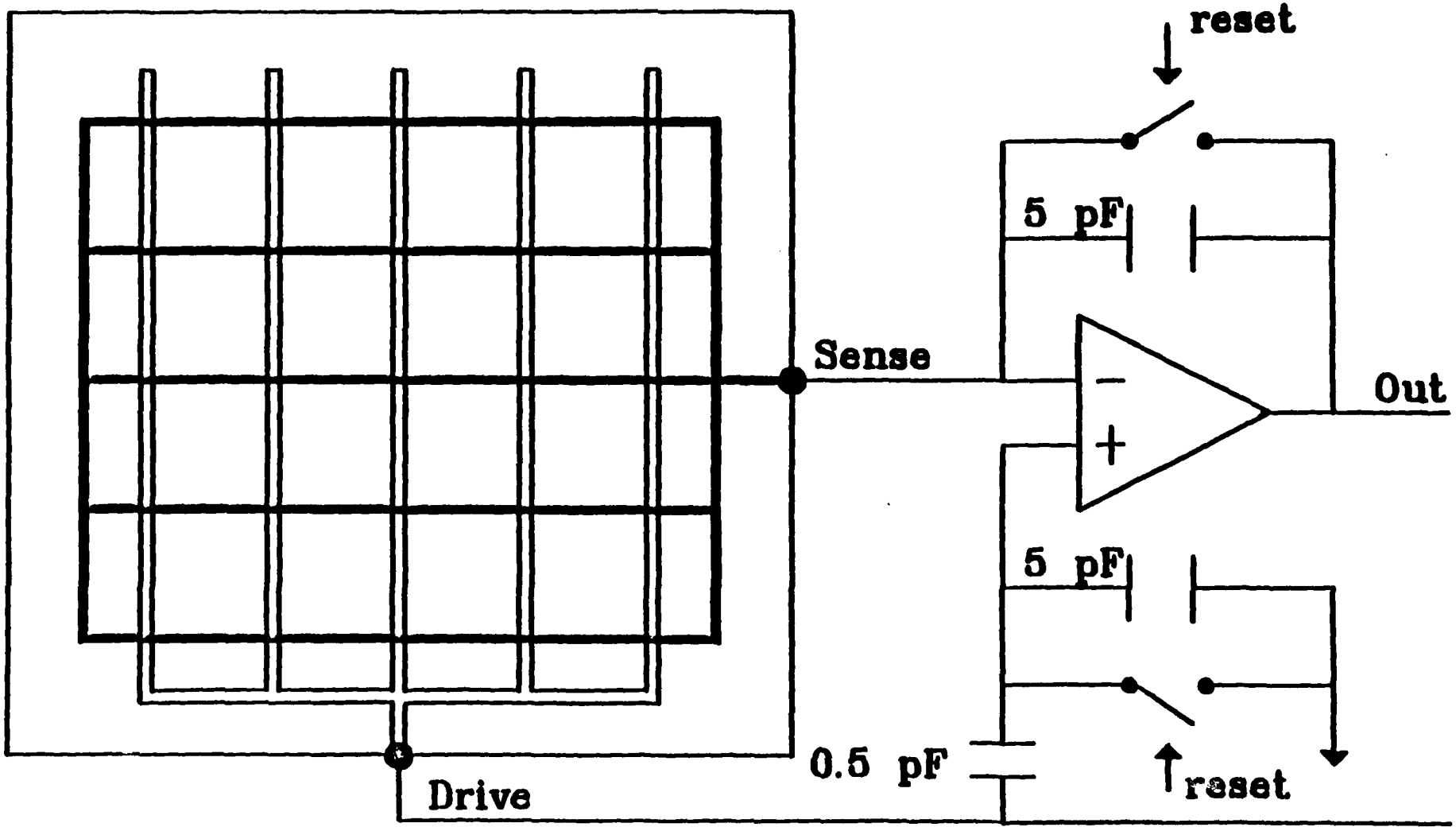

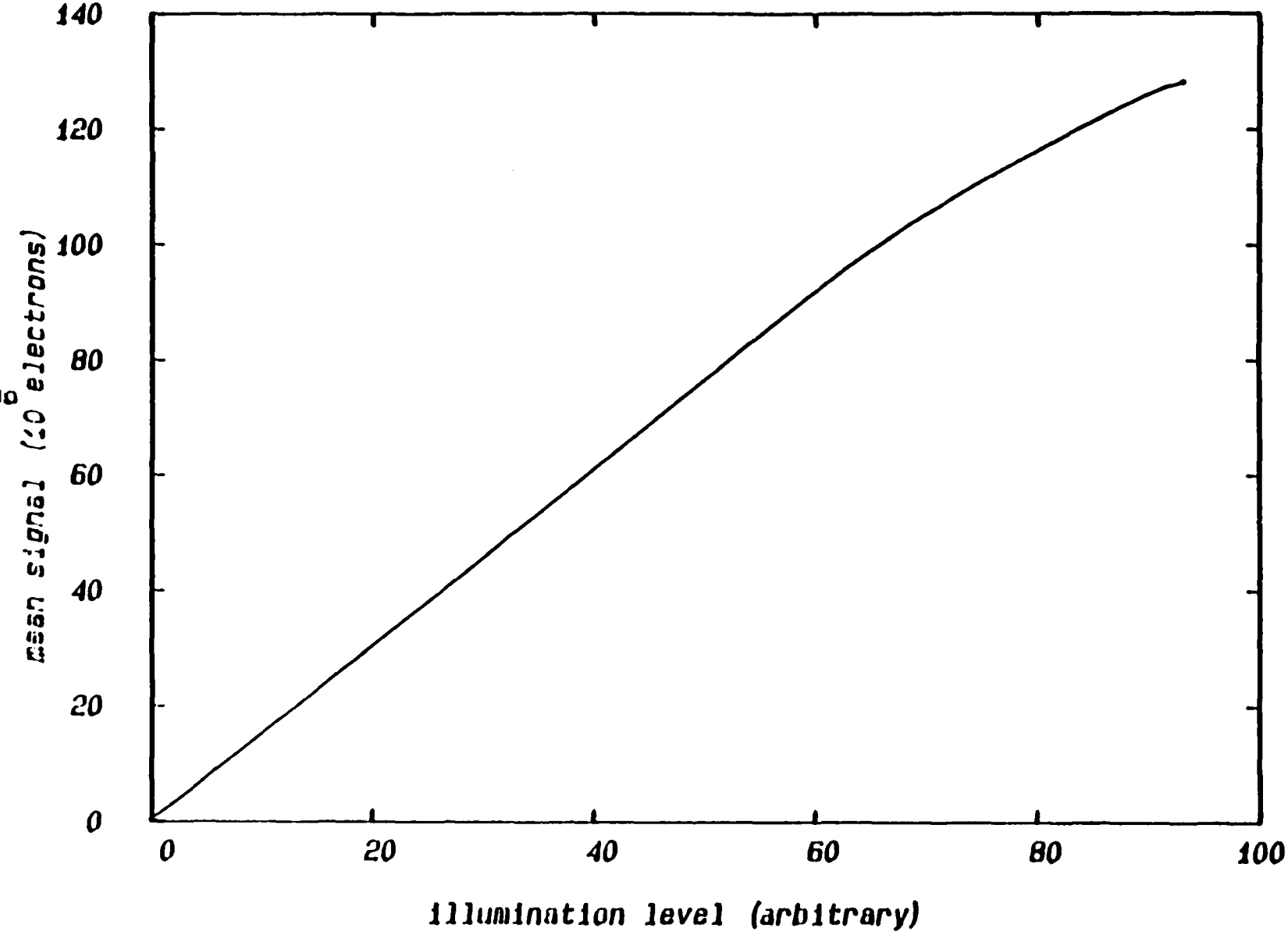
140
120
100
80
60
40
20
0
mean signal (10^6 electrons)
0
20
40
60
80
100
illumination level (arbitrary)

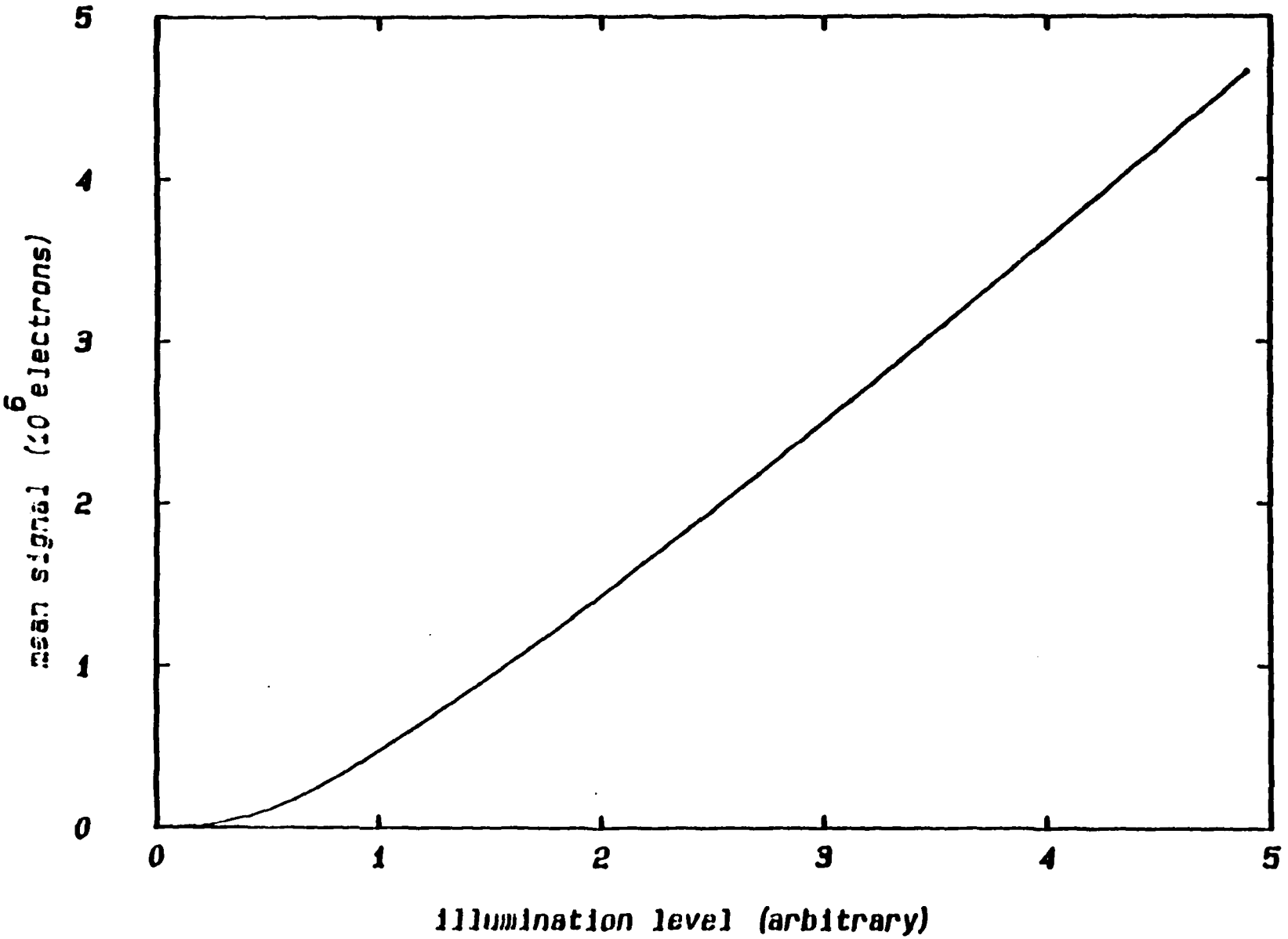
mean signal (10^6 electrons)
0
1
2
3
4
5
0
1
2
3
4
5
illumination level (arbitrary)

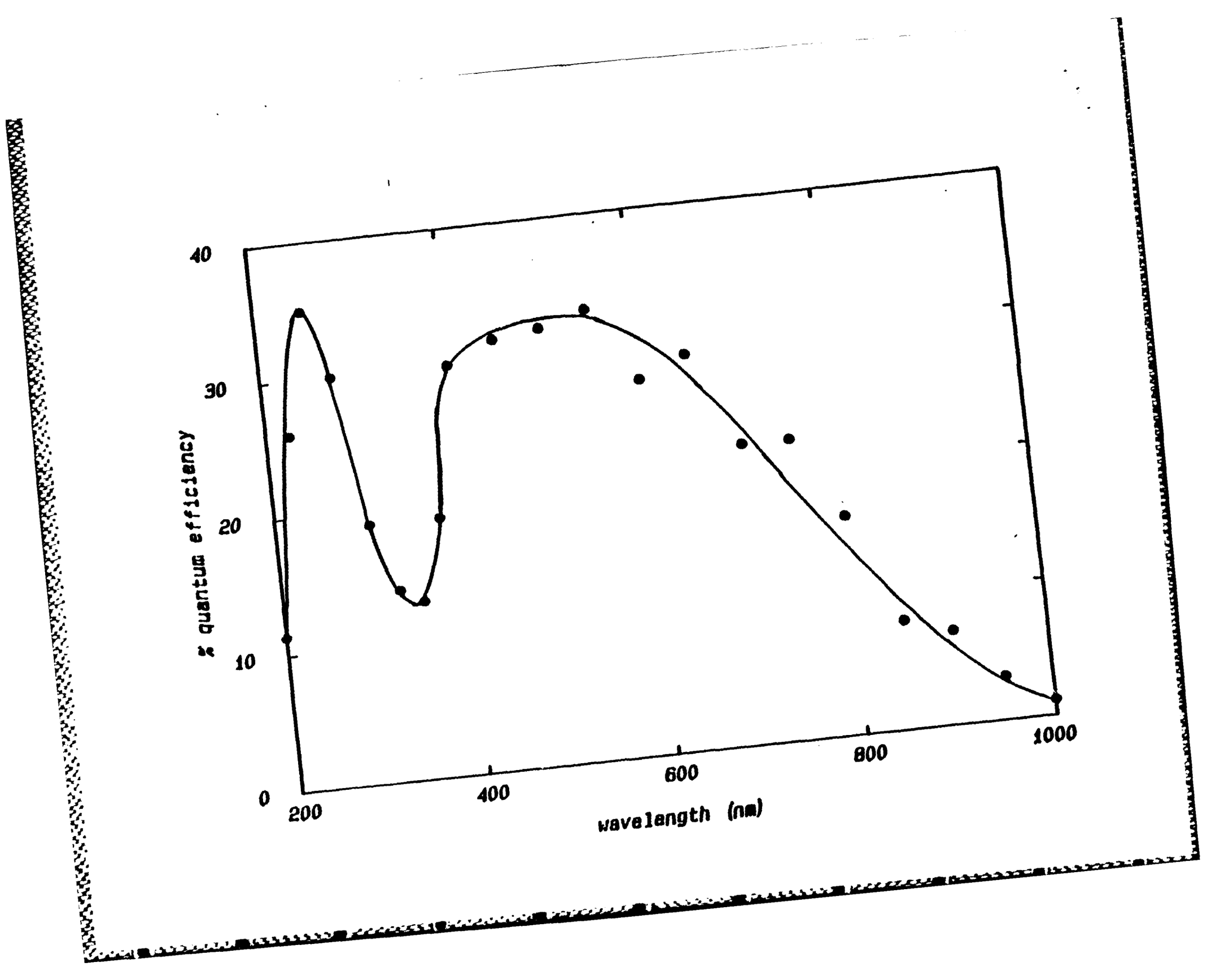
40
30
20
10
0
% quantum efficiency
200
400
600
800
1000
wavelength (nm)

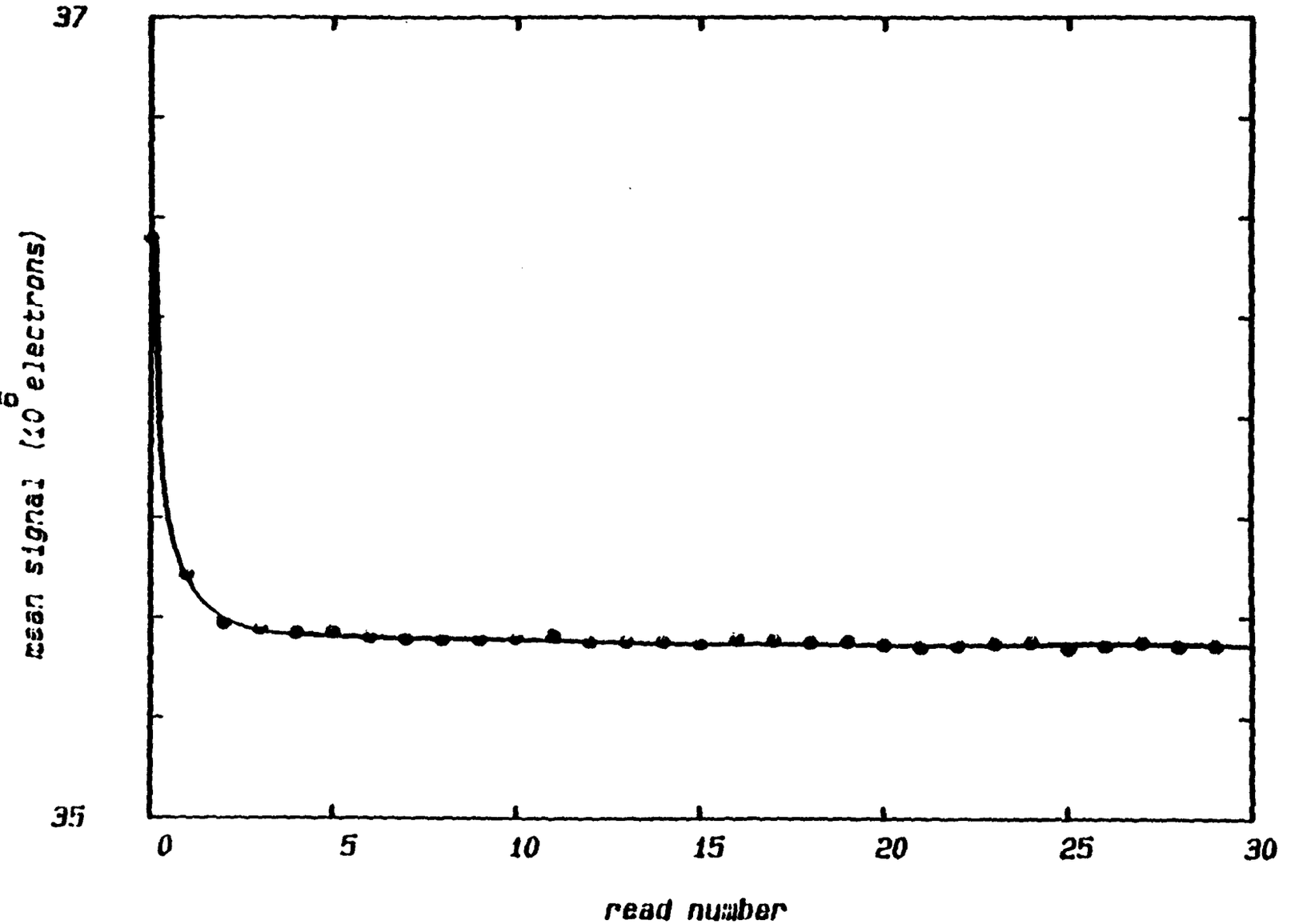
37
35
mean signal (10^6 electrons)
0
5
10
15
20
25
30
read number

TECHNICAL REPORT DISTRIBUTION LIST

	No. Copies
Office of Naval Research Attn: Code 413 800 N. Quincy Street Arlington, Virginia 22217	2
Dr. Bernard Douda Naval Weapons Support Center Code 5042 Crane, Indiana 47522	1
Commander, Naval Air Systems Command Attn: Code 310C (H. Rosenwasser) Washington, D.C. 20360	1
Naval Civil Engineering Laboratory Attn: Dr. R. W. Drisko Port Hueneme, California 93401	1
Defense Technical Information Ctr. Building 5, Cameron Station Alexandria, Virginia 22314	12
DTNSRDC Attn: Dr. G. Bosmajian Applied Chemistry Division Annapolis, Maryland 21401	1
Dr. William Tolles Superintendent Chemistry Division, Code 6100 Naval Research Laboratory Washington, D.C. 20375	1
Dr. David Young Code 334 NORDA NSTL, Mississippi 39529	1
Naval Weapons Center Attn: Dr. Ron Atkins Chemistry Division China Lake, California 93555	1
Scientific Advisor Commandant of the Marine Corps Code RD-1 Washington, D.C. 20380	1
U.S. Army Research Office Attn: CRD-AA-IP P.O. Box 12211 Research Triangle Park, NC 27709	1
Mr. John Boyle Materials Branch Naval Ship Engineering Center Philadelphia, Pennsylvania 19112	1
Naval Ocean Systems Center Attn: Dr. S. Yamamoto Marine Sciences Division San Diego, California 91232	1

END

9-87

DTIC